applied sciences

MDPI

Article

X-ray Photoelectron Spectra of Ag-Au Colloidal Nanoparticles after Interaction with Linear Carbon Chains

Ivan S. Zhidkov [1,2,*], Ernst Z. Kurmaev [1,2], Marcello Condorelli [3], Seif O. Cholakh [1], Alexey S. Boyarchenkov [4], Enza Fazio [5] and Luisa D'Urso [3]

1 Institute of Physics and Technology, Ural Federal University, Mira Street 21, 620002 Yekaterinburg, Russia; ernst.kurmaev@gmail.com (E.Z.K.); s.o.cholakh@urfu.ru (S.O.C.)
2 M.N. Mikheev Institute of Metal Physics, Russian Academy of Sciences, Ural Branch, S. Kovalevskaya Street 18, 620990 Yekaterinburg, Russia
3 Dipartimento di Scienze Chimiche, Universita' di Catania, Viale Andrea Doria 6, 95125 Catania, Italy; marselo88ct@gmail.com (M.C.); ldurso@unict.it (L.D.)
4 Institute of Natural Science, Ural Federal University, Kuibysheva Street 48, 620026 Yekaterinburg, Russia; Alexey.Boyarchenkov@urfu.ru
5 Dipartimento di Scienze Matematiche e Informatiche, Scienze Fisiche e Scienze della Terra, Università degli Studi di Messina, 98166 Messina, Italy; enfazio@unime.it
* Correspondence: i.s.zhidkov@urfu.ru

Abstract: The results of X-ray photoelectron spectra (XPS) characterization of the surface of Ag-Au colloidal nanoparticles (Ag-Au NPs), prepared by laser ablation in water before and after interaction with linear carbon chains (LCC), are presented. No additional features appear in high-energy resolved XPS core level spectra of Ag-Au NPs which indicates that surface is not oxidized. The measurements of XPS Ag 3d-spectrum of (Ag-Au)@LCC manifests the additional low-energy structure that is associated with the formation of Ag–C bonds. The charge transfer between Au atoms on the NPs surface and LCC was established. Additionally, some oxidation of the Ag atoms on the surface of (Ag-Au)@LCC is observed which arises during laser ablation in water. We assume that oxidative species will preferably interact with the areas outside the LCC instead of oxidizing the carbon chains which was confirmed by XPS C 1s spectra.

Keywords: XPS; linear carbon chains; nanoparticles; Ag-Au alloy; electronic structure; oxidation

Citation: Zhidkov, I.S.; Kurmaev, E.Z.; Condorelli, M.; Cholakh, S.O.; Boyarchenkov, A.S.; Fazio, E.; D'Urso, L. X-ray Photoelectron Spectra of Ag-Au Colloidal Nanoparticles after Interaction with Linear Carbon Chains. *Appl. Sci.* **2021**, *11*, 685. https://doi.org/10.3390/app11020685

Received: 9 December 2020
Accepted: 10 January 2021
Published: 12 January 2021

1. Introduction

In recent years, the interest in study of noble metal nanoparticles (NPs) has increased because of their unusual optical properties and chemical stability which is important for their use in optoelectronics [1,2], catalysis [3,4], biosensors [5], and medicine [6,7]. Silver nanoparticles were found to be effective antibacterial substances and can be used as an additive in food [8] and various medical applications [9]. On the other hand, gold NPs are used in microscopy and cancer therapy [10] because of their optical properties. Combining these unique properties in doped nanoparticles of both elements thereby opens up new areas of interest in research and treatment [11]. In this context, the laser ablation Au-Ag alloys in a liquid gives access to colloidal silver-gold alloy NPs with a uniform ultrastructure. For example, the use of silver NPs in combination with gold NPs could open new possibilities for the connection of antibacterial silver nanoparticles to various biomolecules via covalent bonding to gold atoms. To prevent the nanoparticles aggregation and oxidation, the stabilizing species that bind to the nanoparticle surface are crucial.

It was shown recently that linear carbon chains (LCCs) containing *sp*-hybridization are good candidates to create the shell that prevents nanoparticles aggregation and oxidation [12,13]. Despite the fact that long 1D carbon wires (carbine) were first obtained in the laboratory in the 1960s [14] and many methods of their preparation have been proposed to date [15–20], there is still no method that allows one to obtain pure and stable phases of

infinite one-dimensional carbon chains. It is generally accepted that carbyne is unstable due to the exothermic formation of crosslinks between adjacent atomic chains [21]. Significant progress in this area has been achieved with the discovery of polyynes—short sp1 hybridized linear chains with alternating single and triple bonds (–C≡C–C≡C–) [20]. Thus, today there is a sufficient number of studies describing methods of obtaining polyyns and cumulenes (=C=C=C=), as well as methods of their identification. However, the massive synthesis of very long linear carbon chains continues to run into sticking points. However, a number of studies that have appeared in recent years, theoretically and experimentally describing new interesting properties of carbines [22–24], forced to reconsider some approaches to the creation of these materials and renewed interest in them. In particular, it was shown that one-dimensional carbon chains can have a strength, elastic modulus, and stiffness greater than any known material, including diamond, carbon nanotubes, and graphene, and make it possible to create new composite materials [22]. It is also assumed that carbines can be used to create field-effect transistors [25], and also show the possibility of possessing one-dimensional carbon chains with interesting magnetic [26] and electrical properties [27,28].

Taking into account the difficulties caused by the synthesis of linear-chain carbon, it is quite understandable that much attention is currently paid to methods that make it possible to obtain sufficiently stable, albeit not very long structures. In particular, in the last 10–15 years, methods of LCC synthesis on the surface of metal nanoparticles (MeNPs) received widespread attention [12,29,30]. In addition to being able to produce stable LCCs, MeNPs@LCC structures also have a number of additional advantages. Thus, as mentioned before the formation of structures of the core@shell type prevents the agglomeration of nanoparticles in colloidal solutions for a long time, which significantly affects the possibilities of using MeNPs. At the same time, the nature of the chemical interaction between MeNPs and LCC remains unclear, in particular, the stability of LCC on the surface of Ag NPs in water is an unexpected manifestation of such interaction [31]. In the latter case, on the surface of silver nanoparticles, a layer of carbon species several nanometers in size (in *sp* and sp^2 hybridization) was found, sometimes forming a bridge between nanoparticles [12,13]. In hybrid LCC-Me nanostructures, the presence of Me-carbon interactions prevents their degradation, which leads to stable systems for several months [32]. Understanding the nature of this chemical stability will satisfy scientific curiosity and will be very useful in improving the chemical stability of low-dimensional systems.

In this study, we present the results of XPS characterization of Ag-Au and (Ag-Au)@LCC nanoparticles prepared by pulse laser ablation (PLA) in water of great interest for some technological applications in which the control of surface functionalization is fundamental to improve material properties.

2. Materials and Methods

The colloidal solutions of metallic gold and silver were separately produced by pulsed laser ablation (PLA) in Millipore water, using the second harmonic (532 nm) output of a Nd:YAG laser operating at 10 Hz [33,34]. In a second step, Au and Ag colloids were mixed at the volume ratio of 50/50. The as mixed dispersions were obtained from the same parental solutions and irradiated with the same laser source at constant power density (0.2 J/cm^2) and at different irradiation times. The irradiations were performed in order to illuminate the entire system with the same beam. Linear carbon chains (LCCs) containing sp-hybridization as alternating triple and single bonds (polyenes, (–C≡C–)n) were synthesized by arcing between two graphite electrodes in water. Two cylindrical graphite rods (99.995%) with a diameter of about 6 mm were connected to a DC supplier. The voltage was set at 30 V and the measured current was about 10 A. The discharge time was 10 min. The solution of LCCs was filtered with a 0.22 mm filter (Millipore Millex in PES) to remove the large amount of carbon dust formed during the discharge process. To test the formation of Au-Ag nanoalloys the optical transmittance spectrum was immediately recorded, with a double beam spectrophotometer (Perkin-Elmer Lambda

750) through their characteristic absorption peak (400–520 nm). Scanning Transmission Electron Microscopy (STEM) images of kV are shown in Figure 1. Besides coalescence, the lack of an apparent core-shell structure in the STEM picture strongly suggests that the nanoparticles are alloys rather than core-shell composites. Recently Fazio et al. [35] simulated the extinction spectra of Ag-Au alloyed nanoparticles produced by pulsed laser ablation in liquid of elemental targets followed by reirradiation of suitable mixtures of the obtained colloidal suspensions. When we make use of the optical constants of Ag-Au alloys, our theoretical approach, developed in the framework of the T-matrix formalism, accurately reproduces the experimental features of the extinction spectra of laser-produced nanoalloys with compositions that span the entire composition range. Additionally, thanks to the simulation of the optical absorption data, Fazio et al. [35] excluded the formation of core-shell structures and validated the formation of Au-Ag alloys.

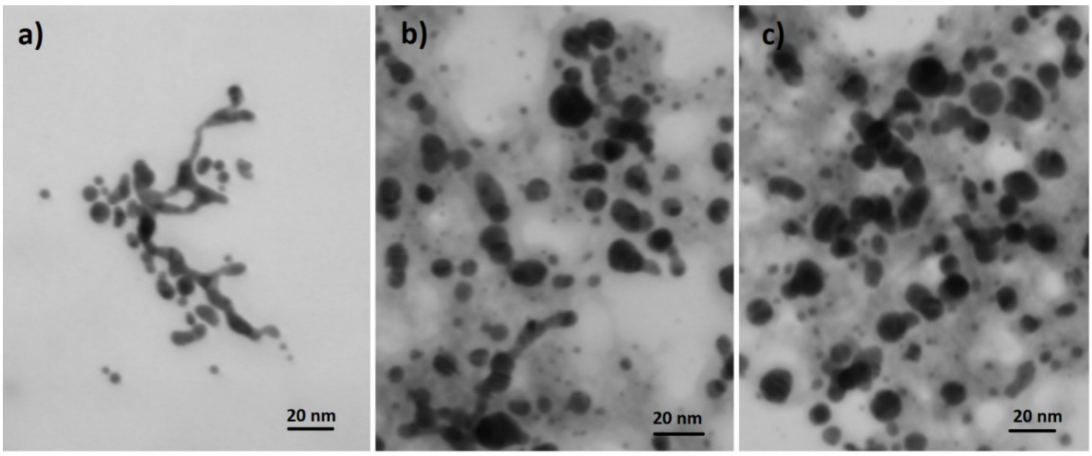

Figure 1. STEM image of the alloy (50:50): (**a**) Au-Ag NPs, (**b**) and (**c**) (Au-Ag)@LCC.

As seen from the histogram (Figure 2) the size of the rounded nanoparticles is about 8 nm and tails down to 2 nm and up to 13 nm.

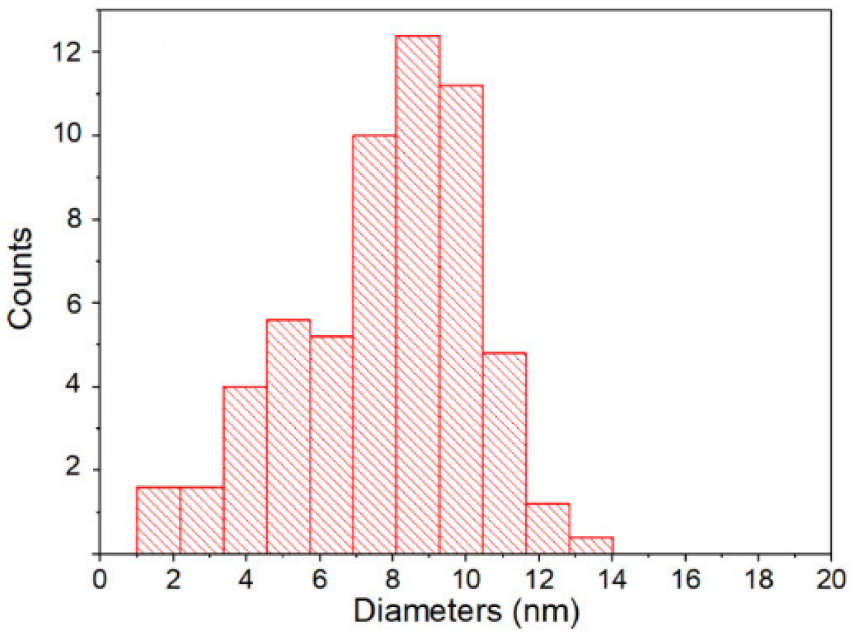

Figure 2. The histogram of Ag/Au@LCC nanoparticles size distribution.

The XPS core-level and valence band (VB) measurements were performed using a PHI 5000 Versa Probe XPS spectrometer (ULVAC Physical Electronics, Chanhassen, MN,

USA) based on a classic X-ray optic scheme with a hemispherical quartz monochromator and an energy analyzer working in the range of binding energies from 0 to 1500 eV. This equipment uses electrostatic focusing and magnetic screening to achieve an energy resolution of $\Delta E \leq 0.5$ eV for Al Kα radiation (1486.6 eV). Pumping of analytical chamber was carried out using an ion pump providing pressure better than 10^{-7} Pa. The XPS spectra were recorded using Al Kα X-ray emission; the spot size was 200 µm, and the X-ray power load delivered to the sample was less than 50 W. Typical signal-to-noise ratios were greater than 10,000:3. XPS spectra were processed using MultiPak 9.9.0.8 software. Finally, the background was taken into account using the Shirley method. A few drops from the nanoparticle suspension was deposited and dried on a monocrystalline silicon substrate to record XPS of the core-levels and valence bands. The presence of metal-carbon bonds is of crucial importance in the solid state analysis since free *sp* chains air-exposed easily degrade as a consequence of their interaction with atmospheric gases [36]. Thus, we are confident that the obtained LCC species on (Ag-Au) nanoparticles are stable and suitable for XPS analysis.

3. Results and Discussion

Figure 3 displays the XPS survey spectra of Ag-Au NPs before and after interaction with LCC. The surface composition determined from these spectra is presented in Table 1. These data show that the concentration of noble materials on the surface of the studied samples does not exceed 0.4 at. %. On this basis we conclude that the NPs were successfully deposited onto silicon substrate despite the fact that concentrations of metal NPs in initial solutions were small enough. The estimated concentration of metal colloids in initial water solution was about 0.3×10^{-6} M. On the other hand, the increasing of carbon concentrations supports the conclusion that LCC structures were also deposited.

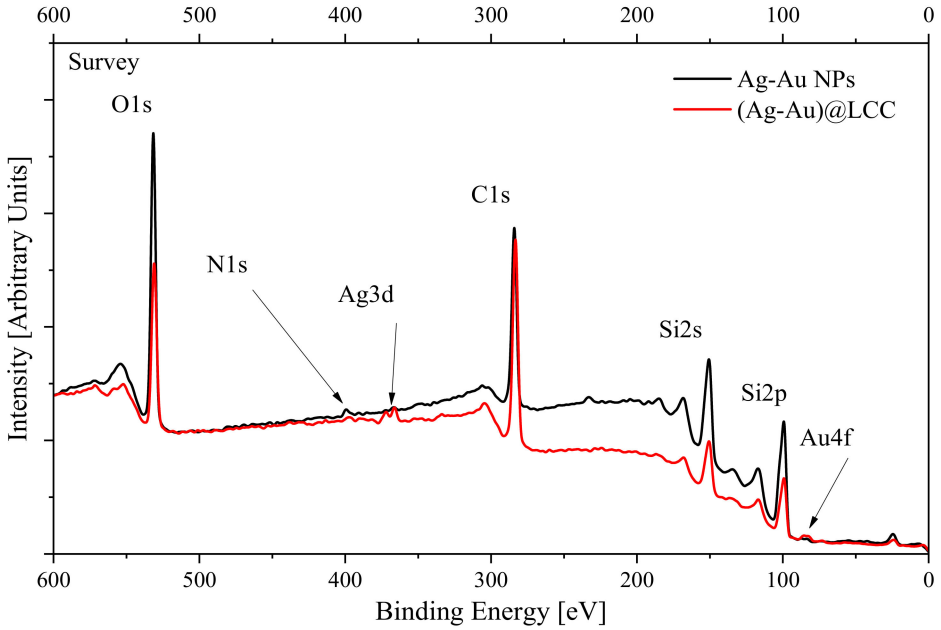

Figure 3. XPS survey spectra of Ag-Au and (Ag-Au)@LCC.

Table 1. Surface composition of Ag-Au and (Ag-Au)@LCC nanoparticles (in at. %).

Sample	C	O	Si	N	Ag	Au
(Ag-Au) NPs	39	31	29.1	0.7	0.1	0.1
(Ag-Au)@LCC	61.8	20.3	16.6	0.8	0.4	0.1

The high-energy resolved XPS Si 2p (Figure 4a) and O 1s-spectra (Figure 4b) of both samples show the main peak (in O 1s) corresponds to Si–O bond in SiO_2. At the same time

Si 2p spectra indicate that the main peak corresponds to Si-Si bond of substrate (99.4 eV) while the feature at 103 eV ascribed to a partial oxidation of the substrate. Further, we should note that an additional low-energy fine structure in the 528.2–531.3 eV energy range appears for (Ag-Au)@LCC. Adsorbed oxygen can contribute to spectral range near 531 eV, however, according to [37,38] the contributions of metal-oxygen bonds (the Ag-O and Au-O) are located at the indicated energy range. This means that a surface oxidation of both metal components in (Ag-Au)@LCC prepared by laser ablation in water could take place. To check this conclusion the high-energy resolved XPS Ag 3d and Au 4f spectra were analyzed (see Figure 5a,b).

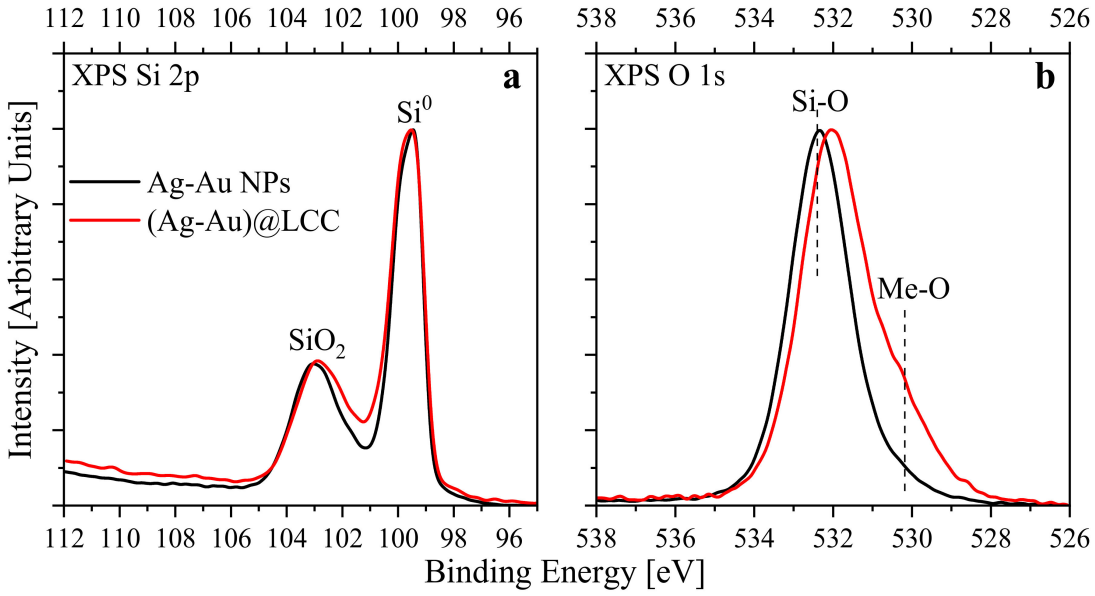

Figure 4. XPS spectra of Ag-Au and (Ag-Au)@LCC: (**a**) Si2p and (**b**) O 1s.

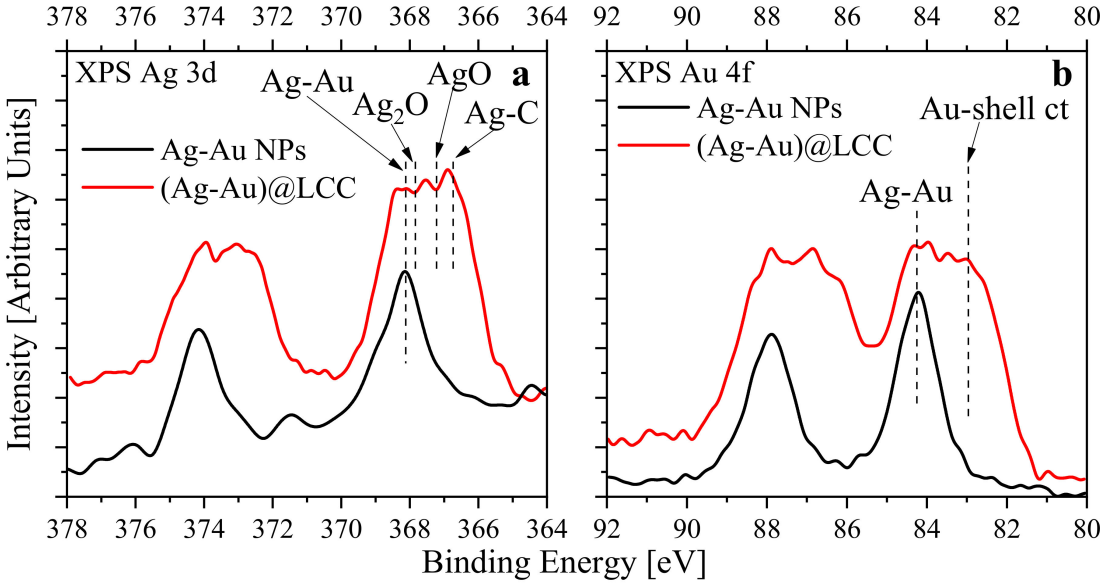

Figure 5. XPS spectra of Ag-Au and (Ag-Au)@LCC: (**a**) Ag 3d and (**b**) Au 4f. Label "Au-shell ct" designates charge transfer between Au atoms and LCCs shell.

It emerged that the spectra of both components for (Ag-Au)@LCC nanoparticles show a two-peak structure. In details, XPS spectra of Ag $3d_{5/2,3/2}$ (Figure 5a) shows lines at the binding energies of 366.7 and 372.6 eV. We should note that the Ag $3d_{5/2}$ lineshape

between 366.7 and 368.2 eV could arise from Ag–O bonds (specifically, Ag $3d_{5/2}$ located at 367.33 eV for AgO [37] and at 367.62 eV for Ag_2O [39]). However, these additional lines cannot be attributed only to oxidation of (Ag-Au)@LCC nanoparticles since XPS Ag 3d lines in oxides have higher binding energies in XPS spectra than 366.7 eV peak. Earlier it was shown that this feature could arise from the formation of Ag–C bond in Ag@LCC NPs [40] and Ag NPs [41] and nanowires [42]. Moreover, we do not exclude that, during the second irradiation, a series of Ag or Au end-capped LCCs are also formed together to the Ag NPs encapsulated in carbonaceous shells [40]. On the other hand, the additional feature appearing at lower binding energy might hint of the electron transfer to Au.

A similar picture could be seen in Au 4f spectra (Figure 5b) where the presence of a low energy band could be associated with Au and C atoms interaction because the similar peaks were observed in the Au 4f spectra of Au@LCC [43]. The lower-energy shift of Au 4f peak position is a known for metal nanoparticles (including Au) on various substrates [44–47] due to strong metal–substrate interactions. It should be noted that some authors refer to the low-energy shift to negatively charged gold atoms organized in clusters [48]. Liu et al. [49] associated the same shift of Au 4f binding energies for Au-Pd NPs (Au core–Pd shell) to an increase in the surface to volume ratio as the Au core became smaller. In our case we suggest that gold atoms located at NPs surface strongly interacted with LCC shell. For this reason, the gold atoms located on the NPs surfaces show a significant shift to lower binding energy while atoms located in the core of NPs show the peak position close to the Ag-Au alloy. Such electronic properties of (Ag-Au)@LCC NPs provide the opportunities to develop the novel catalytic systems with unusual properties.

However, unlike the Ag 3d spectra, the formation of the Au–O bond could not be confirmed with certainty since, in the Au $4f_{7/2,5/2}$ spectra, Au_2O_3 peaks are shifted to an opposite side to 85.9 and 89.5 eV [50,51]. Otherwise, the formation of Ag–C and Au–C bonds are also evidenced by XPS C 1s spectra (Figure 6) where their low-energy features are detected for (Ag-Au)@LCC structure. It should be noted that C 1s line for pure LCC is also located at the same energy region [52] of the (Ag-Au)@LCC sample. Due to relatively low concentrations of metal nanoparticles, we conclude that the main contribution to this energy range arises from carbon-carbon *sp*-hybridized bonds in LCC. This result is important because it indicates the stability of the obtained LCC which is crucial for their applications. We did not observe the signals referred to C–O and (C=O) bonds, generally observed at higher binding energy with respect to C–C bonds in the C 1s lineshape. Thus, we can conclude that the linear carbon chains in investigated samples are not oxidized.

The observed two-peak structure of the XPS Ag 3d and Au 4f-spectra is absent in Ag-Au NPs. This confirms the conclusions about the formation of bonds between LCC and Ag/Au atoms. It is important to note that the binding energies of high-energy peaks differ from those in pure metals [53] and are close to the energies of Ag-Au alloys [54]. This leads to the conclusion that the used method of sample preparation ensures the formation of Ag-Au alloy nanoparticles.

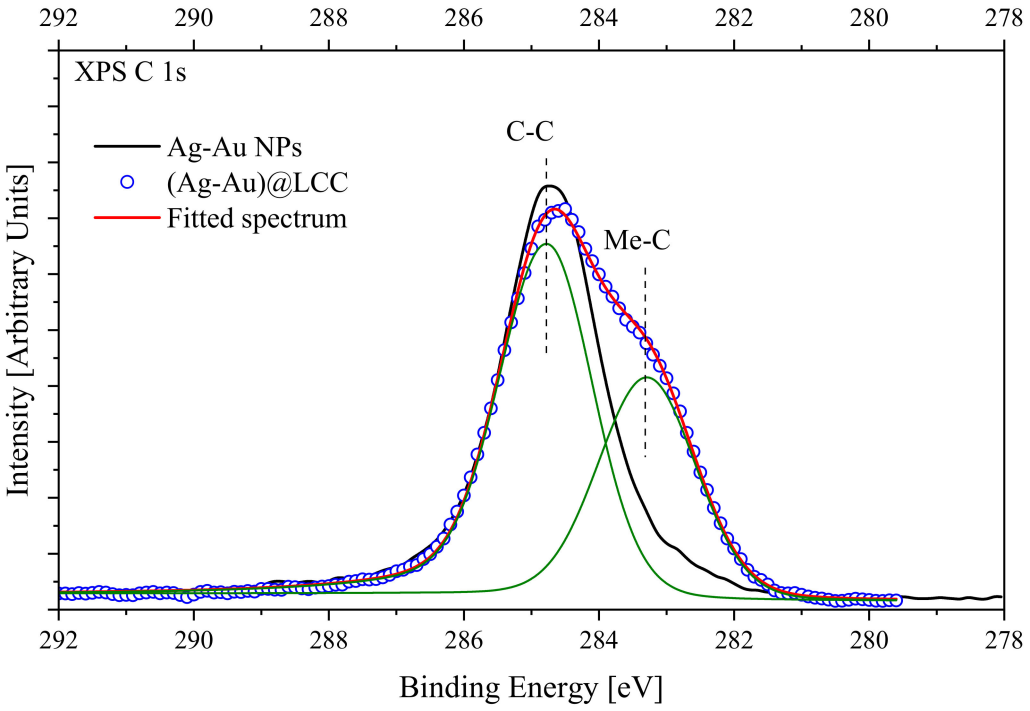

Figure 6. XPS C 1s spectra of Ag-Au and (Ag-Au)@LCC.

4. Conclusions

The nanostructured core@shell composites, in which the inner noble metal nanoparticle is encapsulated and protected from agglomeration, adsorption, or chemical reactions by the outer shell, attract a lot of attention due to their unique physical, chemical, biological, and catalytic properties. The thickness of the outer shell plays a huge role in the formation of the functional properties of nanocomposites and, therefore, the nanometer scale, which can be implemented using carbon materials with one or several layers, is of particular interest. The use of two successive processes during ablation, that is the formation of noble metal nanoparticles and subsequent carbon deposition, allows to obtain noble metal nanoparticles in a homogeneous and ultrathin carbon layer. In the present work, the surface of Ag-Au alloys colloidal nanoparticles, obtained by laser ablation in water was characterized by XPS and the formation of Ag–C bonds was established. We found low-energy chemical shift for the Au 4f doublet which has previously been observed for Au NPs on different substrates. Despite the existence of various interpretations of such a shift in the literature, we assume that low-energy shift of Au 4f levels in (Ag-Au)@LCC could be attributed to a size-induced gold-LCC charge transfer. It is shown that agglomeration can be eliminated by the interaction of colloidal nanoparticles with linear carbon chains and formation of (Ag-Au)@LCC nanostructures.

Author Contributions: Conceptualization, E.Z.K. and L.D.; methodology, I.S.Z. and L.D.; formal analysis, I.S.Z., E.Z.K. and L.D.; investigation, I.S.Z., M.C., S.O.C., A.S.B. and E.F.; resources, S.O.C. and L.D.; writing—original draft preparation, E.Z.K. and I.S.Z.; writing—review and editing, I.S.Z., E.Z.K., E.F. and L.D.; supervision, S.O.C., E.Z.K. and L.D.; funding acquisition, I.S.Z. and E.Z.K. All authors have read and agreed to the published version of the manuscript.

Funding: This study was supported by Russian Science Foundation (Project 19-72-00001). E.Z.K. and S.O.C. thank Ministry of Science and High Education of Russia (Theme "Electron" No. AAAA-A18–118020190098-5 and Project FEUZ-2020–0060) for financial support.

Data Availability Statement: Data is contained within the article.

Conflicts of Interest: The authors declare no conflict of interest.

References

1. Xie, B.; Ma, L.; Zhao, J.; Liu, L. Dependent absorption property of nanoparticle clusters: An investigation of the competing effects in the near field. *Opt. Express* **2019**, *27*, A280–A291. [CrossRef]
2. Abdelhalim, M.A.K.; Mady, M.M.; Ghannam, M.M. Physical Properties of Different Gold Nanoparticles: Ultraviolet-Visible and Fluorescence Measurements. *J. Nanomed. Nanotechnol.* **2012**, *3*, 133. [CrossRef]
3. Stratakis, M.; García, H. Catalysis by Supported Gold Nanoparticles: Beyond Aerobic Oxidative Processes. *Chem. Rev.* **2012**, *112*, 4469–4506. [CrossRef]
4. Bond, G.C. Hydrogenation by gold catalysts: An unexpected discovery and a current assessment. *Gold Bull.* **2016**, *49*, 53–61. [CrossRef]
5. Li, Y.; Schluesener, H.J.; Xu, S. Gold nanoparticle-based biosensors. *Gold Bull.* **2010**, *43*, 29–41. [CrossRef]
6. Arvizo, R.R.; Bhattacharyya, S.; Kudgus, R.A.; Giri, K.; Bhattacharya, R.; Mukherjee, P. Intrinsic therapeutic applications of noble metal nanoparticles: Past, present and future. *Chem. Soc. Rev.* **2012**, *41*, 2943–2970. [CrossRef]
7. Dykman, L.; Khlebtsov, N. Gold nanoparticles in biomedical applications: Recent advances and perspectives. *Chem. Soc. Rev.* **2012**, *41*, 2256–2282. [CrossRef]
8. Ortega, F.; Garcia, M.A.; Arce, V.B. Nanocomposite films with silver nanoparticles synthesized in situ: Effect of corn starch content. *Food Hydrocoll.* **2019**, *97*, 105200. [CrossRef]
9. Amini, S.M. Preparation of antimicrobial metallic nanoparticles with bioactive compounds. *Mater. Sci. Eng. C* **2019**, *103*, 109809. [CrossRef]
10. Liao, J.; Jia, Y.; Chen, L.; Zhou, L.; Li, Q.; Qian, Z.; Niu, D.; Li, Y.; Li, P. Magnetic/Gold Core-Shell Hybrid Particles for Targeting and Imaging-Guided Photothermal Cancer Therapy. *J. Biomed. Nanotechnol.* **2019**, *15*, 2072–2089. [CrossRef]
11. Grade, S.; Eberhard, J.; Jakobi, J.; Winkel, A.; Stiesch, M.; Barcikowski, S. Alloying colloidal silver nanoparticles with gold disproportionally controls antibacterial and toxic effects. *Gold Bull.* **2013**, *47*, 83–93. [CrossRef]
12. D'Urso, L.; Grasso, G.; Messina, E.; Bongiorno, C.; Scuderi, V.; Scalese, S.; Puglisi, O.; Spoto, G.; Compagnini, G. Role of Linear Carbon Chains in the Aggregation of Copper, Silver, and Gold Nanoparticles. *J. Phys. Chem. C* **2009**, *114*, 907–915. [CrossRef]
13. Grasso, G.; D'Urso, L.; Messina, E.; Cataldo, F.; Puglisi, O.; Spoto, G.; Compagnini, G. A mass spectrometry and surface enhanced Raman spectroscopy study of the interaction between linear carbon chains and noble metals. *Carbon* **2009**, *47*, 2611–2619. [CrossRef]
14. Kasatochkin, V.I.; Sladkov, A.M.; Kudryavtsev, Y.P.; Popov, N.M.; Korshak, V.V. Crystalline forms of a linear modification of carbon. *Dokl. Akad. Nauk SSSR* **1967**, *117*, 358–360.
15. Cataldo, F. Synthesis of polyynes in a submerged electric arc in organic solvents. *Carbon* **2004**, *42*, 129–142. [CrossRef]
16. Tsuji, M.; Kuboyama, S.; Matsuzaki, T.; Tsuji, T. Formation of hydrogen-capped polyynes by laser ablation of C60 particles suspended in solution. *Carbon* **2003**, *41*, 2141–2148. [CrossRef]
17. Khanna, R.; Ikram-Ul-Haq, M.; Rawal, A.; Rajarao, R.; Sahajwalla, V.; Cayumil, R.; Mukherjee, P.S. Formation of carbyne-like materials during low temperature pyrolysis of lignocellulosic biomass: A natural resource of linear sp carbons. *Sci. Rep.* **2017**, *7*, 16832. [CrossRef]
18. Olejniczak, A.; Nebogatikova, N.A.; Frolov, A.; Kulik, M.; Antonova, I.V.; Skuratov, V.A. Swift heavy-ion irradiation of graphene oxide: Localized reduction and formation of sp-hybridized carbon chains. *Carbon* **2019**, *141*, 390–399. [CrossRef]
19. Casari, C.S.; Tommasini, M.; Tykwinski, R.R.; Milani, A. Carbon-atom wires: 1-D systems with tunable properties. *Nanoscale* **2016**, *8*, 4414–4435. [CrossRef]
20. Chalifoux, W.A.; Tykwinski, R.R. Synthesis of polyynes to model the sp-carbon allotrope carbyne. *Nat. Chem.* **2010**, *2*, 967–971. [CrossRef]
21. La Torre, A.; Mendez, A.R.B.; Baaziz, W.; Charlier, J.-C.; Banhart, F. Strain-induced metal–semiconductor transition observed in atomic carbon chains. *Nat. Commun.* **2015**, *6*, 6636. [CrossRef] [PubMed]
22. Liu, M.; Artyukhov, V.I.; Lee, H.; Xu, F.; Yakobson, B.I. Carbyne from First Principles: Chain of C Atoms, a Nanorod or a Nanorope. *ACS Nano* **2013**, *7*, 10075–10082. [CrossRef] [PubMed]
23. Casillas, G.; Mayoral, A.; Liu, M.; Ponce, A.; Artyukhov, V.I.; Yakobson, B.I.; José-Yacamán, M. New insights into the properties and interactions of carbon chains as revealed by HRTEM and DFT analysis. *Carbon* **2014**, *66*, 436–441. [CrossRef] [PubMed]
24. Kutrovskaya, S.; Osipov, A.; Baryshev, S.; Zasedatelev, A.; Samyshkin, V.; Demirchyan, S.; Pulci, O.; Grassano, D.; Gontrani, L.; Hartmann, R.R.; et al. Excitonic Fine Structure in Emission of Linear Carbon Chains. *Nano Lett.* **2020**, *20*, 6502–6509. [CrossRef]
25. Baughman, R.H. Chemistry: Dangerously Seeking Linear Carbon. *Science* **2006**, *312*, 1009–1110. [CrossRef]
26. Wong, C.H.; Buntov, E.A.; Zatsepin, A.F.; Lyu, J.; Lortz, R.; Zatsepin, D.A.; Guseva, M.B. Room temperature p-orbital magnetism in carbon chains and the role of group IV, V, VI, and VII dopants. *Nanoscale* **2018**, *10*, 11186–11195. [CrossRef]
27. Wong, C.; Buntov, E.; Guseva, M.; Kasimova, R.; Rychkov, V.; Zatsepin, A. Superconductivity in ultra-thin carbon nanotubes and carbyne-nanotube composites: An ab-initio approach. *Carbon* **2017**, *125*, 509–515. [CrossRef]
28. Buntov, E.; Zatsepin, A.; Slesarev, A.; Shchapova, Y.; Challinger, S.; Baikie, I. Effect of thickness and substrate type on the structure and low vacuum photoemission of carbyne-containing films. *Carbon* **2019**, *152*, 388–395. [CrossRef]
29. Kucherik, A.O.; Osipov, A.V.; Arakelian, S.M.; Garnov, S.V.; Povolotckaya, A.V.; Kutrovskaya, S.V. The laser-assisted synthesis of linear carbon chains stabilized by noble metal particle. *J. Phys. Conf. Ser.* **2019**, *1164*, 012006. [CrossRef]

30. Arakelyan, S.M.; Veiko, V.P.; Kutrovskaya, S.V.; Kucherik, A.; Osipov, A.V.; Vartanyan, T.A.; Itina, T. Reliable and well-controlled synthesis of noble metal nanoparticles by continuous wave laser ablation in different liquids for deposition of thin films with variable optical properties. *J. Nanopart. Res.* **2016**, *18*, 1–12. [CrossRef]
31. Shen, A.; Chen, L.; Xie, W.; Hu, J.; Zeng, A.; Richards, R.; Hu, J. Triplex Au-Ag-C Core-Shell Nanoparticles as a Novel Raman Label. *Adv. Funct. Mater.* **2010**, *20*, 969–975. [CrossRef]
32. Casari, C.S.; Russo, V.; Bassi, A.L.; Bottani, C.E.; Cataldo, F.; Lucotti, A.; Tommasini, M.; Del Zoppo, M.; Castiglioni, C.; Zerbi, G. Stabilization of linear carbon structures in a solid Ag nanoparticle assembly. *Appl. Phys. Lett.* **2007**, *90*, 013111. [CrossRef]
33. Compagnini, G.; Messina, E.; Puglisi, O.; Nicolosi, V. Laser synthesis of Au/Ag colloidal nano-alloys: Optical properties, structure and composition. *Appl. Surf. Sci.* **2007**, *254*, 1007–1011. [CrossRef]
34. Compagnini, G.; Messina, E.; Puglisi, O.; Cataliotti, R.S.; Nicolosi, V. Spectroscopic evidence of a core–shell structure in the earlier formation stages of Au–Ag nanoparticles by pulsed laser ablation in water. *Chem. Phys. Lett.* **2008**, *457*, 386–390. [CrossRef]
35. Fazio, E.; Saija, R.; Santoro, M.; Abir, S.; Neri, F.; Tommasini, M.; Ossi, P.M. On the Optical Properties of Ag–Au Colloidal Alloys Pulsed Laser Ablated in Liquid: Experiments and Theory. *J. Phys. Chem. C* **2020**, *124*, 24930–24939. [CrossRef]
36. D'Urso, L.; Compagnini, G.; Puglisi, O. sp/sp2 bonding ratio in sp rich amorphous carbon thin films. *Carbon* **2006**, *44*, 2093–2096. [CrossRef]
37. Kaspar, T.C.; Droubay, T.; Chambers, S.A.; Bagus, P.S. Spectroscopic Evidence for Ag(III) in Highly Oxidized Silver Films by X-ray Photoelectron Spectroscopy. *J. Phys. Chem. C* **2010**, *114*, 21562–21571. [CrossRef]
38. Irissou, E.; Denis, M.-C.; Chaker, M.; Guay, D. Gold oxide thin film grown by pulsed laser deposition in an O_2 atmosphere. *Thin Solid Films* **2005**, *472*, 49–57. [CrossRef]
39. Weaver, J.F.; Hoflund, G.B. Surface Characterization Study of the Thermal Decomposition of Ag_2O. *Chem. Mater.* **1994**, *6*, 1693–1699. [CrossRef]
40. Bukhvalov, D.W.; Zhidkov, I.S.; Kurmaev, E.Z.; Fazio, E.; Cholakh, S.; D'Urso, L. Atomic and electronic structures of stable linear carbon chains on Ag-nanoparticles. *Carbon* **2018**, *128*, 296–301. [CrossRef]
41. Kawai, K.; Narushima, T.; Kaneko, K.; Kawakami, H.; Matsumoto, M.; Hyono, A.; Nishihara, H.; Yonezawa, T. Synthesis and antibacterial properties of water-dispersible silver nanoparticles stabilized by metal–carbon σ-bonds. *Appl. Surf. Sci.* **2012**, *262*, 76–80. [CrossRef]
42. Bashouti, M.Y.; Resch, S.; Ristein, J.; Mačković, M.; Spiecker, E.; Waldvogel, S.R.; Christiansen, S. Functionalization of Silver Nanowires Surface using Ag–C Bonds in a Sequential Reductive Method. *ACS Appl. Mater. Interfaces* **2015**, *7*, 21657–21661. [CrossRef] [PubMed]
43. Zhidkov, I.S.; Kurmaev, E.Z.; Cholakh, S.O.; Fazio, E.; D'Urso, L. XPS study of interactions between linear carbon chains and colloidal Au nanoparticles. *Mendeleev Commun.* **2020**, *30*, 285–287. [CrossRef]
44. Song, Z.; Li, W.; Niu, F.; Xu, Y.; Niu, L.; Yang, W.; Wang, Y.; Liu, J. A novel method to decorate Au clusters onto graphene via a mild co-reduction process for ultrahigh catalytic activity. *J. Mater. Chem. A* **2017**, *5*, 230–239. [CrossRef]
45. Yang, K.; Meng, C.; Lin, L.; Peng, X.; Chen, X.; Wang, X.; Dai, W.; Fu, X. A heterostructured TiO2–C3N4 support for gold catalysts: A superior preferential oxidation of CO in the presence of H2 under visible light irradiation and without visible light irradiation. *Catal. Sci. Technol.* **2016**, *6*, 829–839. [CrossRef]
46. Hsiao, Y.-P.; Su, W.-Y.; Cheng, J.-R.; Cheng, S.-H. Electrochemical determination of cysteine based on conducting polymers/gold nanoparticles hybrid nanocomposites. *Electrochim. Acta* **2011**, *56*, 6887–6895. [CrossRef]
47. Nascente, P.; Maluf, S.S.; Afonso, C.R.; Landers, R.; Pinheiro, A.; Leite, E. Au and Pd nanoparticles supported on CeO 2, TiO 2, and Mn_2O_3 oxides. *Appl. Surf. Sci.* **2014**, *315*, 490–498. [CrossRef]
48. Apostol, N.G.; Stoflea, L.E.; Lungu, G.-A.; Chirilă, C.; Trupina, L.; Negrea, R.; Ghica, C.; Pintilie, L.; Teodorescu, C.M. Charge transfer and band bending at Au/Pb(Zr0.2Ti0.8)O3 interfaces investigated by photoelectron spectroscopy. *Appl. Surf. Sci.* **2013**, *273*, 415–425. [CrossRef]
49. Liu, F.; Wechsler, D.; Zhang, P. Alloy-structure-dependent electronic behavior and surface properties of Au–Pd nanoparticles. *Chem. Phys. Lett.* **2008**, *461*, 254–259. [CrossRef]
50. Juodkazis, K. XPS studies on the gold oxide surface layer formation. *Electrochem. Commun.* **2000**, *2*, 503–507. [CrossRef]
51. Tchaplyguine, M.; Mikkelä, M.-H.; Zhang, C.; Andersson, T.; Björneholm, O. Gold Oxide Nanoparticles with Variable Gold Oxidation State. *J. Phys. Chem. C* **2015**, *119*, 8937–8943. [CrossRef]
52. Danno, T.; Okada, Y.; Kawaguchi, J. XPS Study of Carbyne-Like Carbon Films. *AIP Conf. Proc.* **2014**, *723*, 431.
53. Moulder, J.F.; Stickle, W.F.; Sobol, P.E.; Bomben, K.D. *Handbook of X-ray Photoelectron Spectroscopy*; Chastain, J., King, R.C.J., Eds.; ULVAK-PHI, Inc.: Chanhassen, MN, USA, 1995.
54. Wang, A.-Q.; Liu, J.-H.; Lin, S.; Lin, T.-S.; Mou, C. A novel efficient Au–Ag alloy catalyst system: Preparation, activity, and characterization. *J. Catal.* **2005**, *233*, 186–197. [CrossRef]